

Supporting Information

Synthesis, characterization and oxygen atom transfer reactivity of a pair of Mo(IV)O- and Mo(VI)O₂-enedithiolate complexes – a look at both ends of the catalytic transformation

Ashta C. Ghosh,^a Prinson P. Samuel,^b Carola Schulzke^c

^aInstitute of Condensed Matter and Nanosciences, Molecules, Solids and Reactivity (IMCN/MOST), Université catholique de Louvain, Place L. Pasteur 1, 1348 Louvain-la-Neuve, Belgium. E-mail: ashtajchem@gmail.com

^bUniversität Göttingen, Institut für Anorganische Chemie, Tammannstr. 4, 37077 Göttingen, Germany.

^cInstitut für Biochemie, Ernst-Moritz-Arndt-Universität Greifswald, Felix-Hausdorff-Strasse 4, 17487 Greifswald, Germany. E-mail: carola.schulzke@uni-greifswald.de

Table S1. Crystal Data and Structure Refinement Parameters for **1**.

parameters	(Bu ₄ N) ₂ [MoO(ntdt) ₂] (1)
formula	C ₅₆ H ₈₈ MoN ₂ OS ₄
formula weight	1029.46
crystal system	Orthorhombic
space group	P2 ₁ 2 ₁ 2 ₁
Z	4
a, Å	14.281(3)
b, Å	14.491(3)
c, Å	27.124(5)
$\alpha = \beta = \gamma$, deg	90.00
V, Å ³	5613(2)
T, K	133(2)
$\lambda(\text{Mo}_{\text{K}\alpha})$, Å	0.71073
μ, mm^{-1}	0.420
D_{calcd} , g/cm ³	1.218
F (000)	2208
reflections [$ I > 2\sigma(I)$]	9861
unique reflections	10862
measured reflections	49904
R_{int}	0.0378
GOF on F^2	1.010
$R_1^{[a]}$, $R_w^{[b]}$ [$ I > 2\sigma(I)$]	0.0305, 0.0690
R_1 , R_w (all data)	0.0362. 0.0706
$\Delta\rho$ max/min [e Å ⁻³]	0.414, -0.277

^[a] $R_1 = \sum |F_o| - |F_c| | / \sum |F_o|$; ^[b] $R_w = [\sum \{w(F_o^2 - F_c^2)^2\} / \sum \{w(F_o^2)^2\}]^{1/2}$

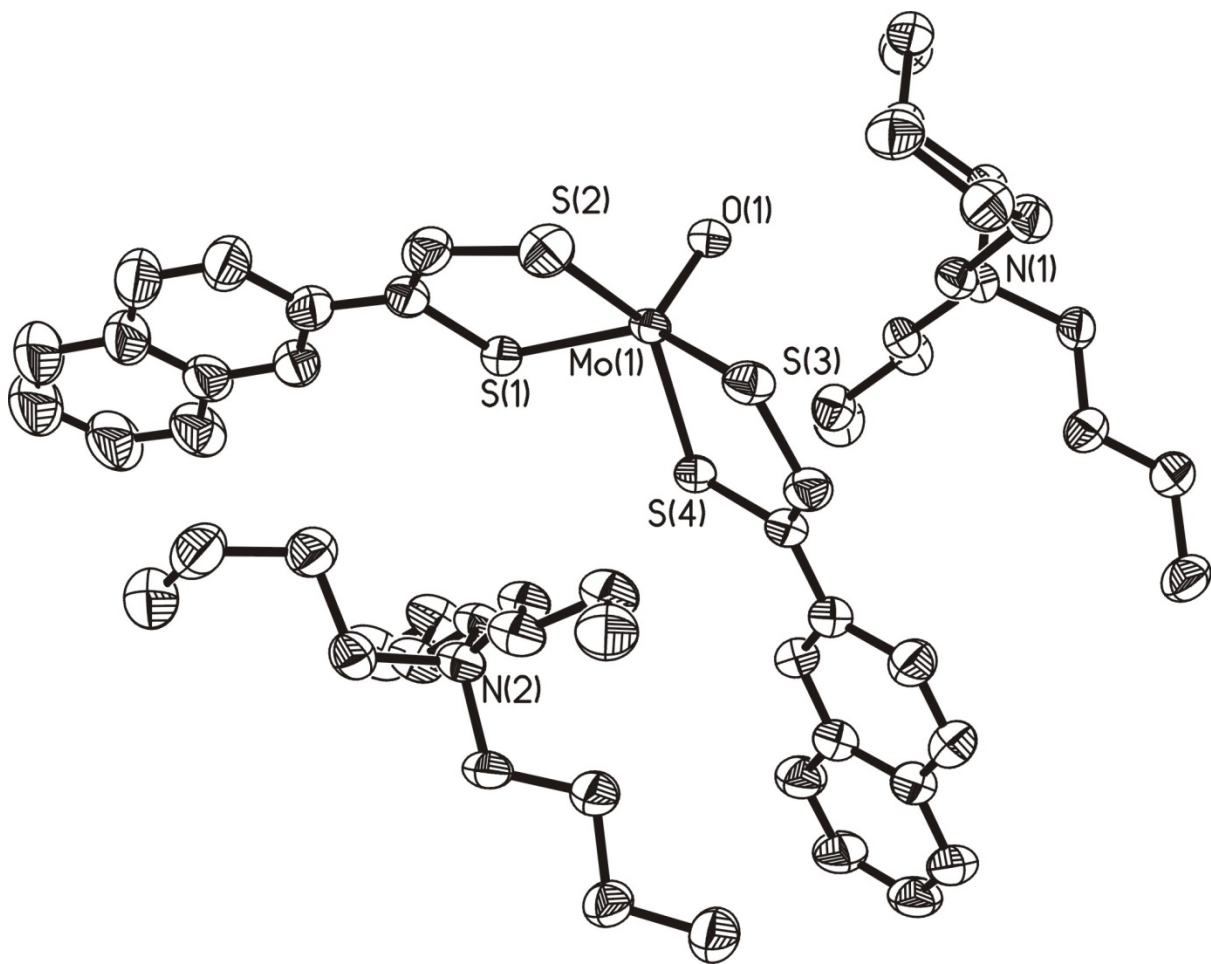


Figure S1. Molecular structure of $[Bu_4N]_2[MoO(ntdt)_2]$ (1) with 50% probability thermal ellipsoids.

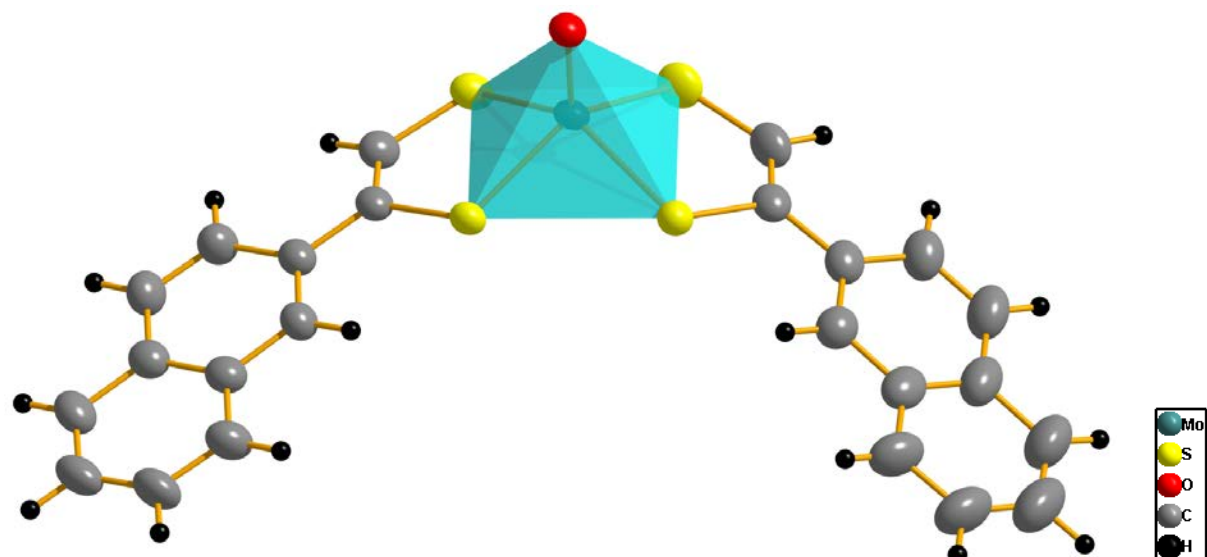


Figure S2. Molecular structure of the dianion of $[Bu_4N]_2[MoO(ntdt)_2]$ (1) showing the square-based pyramidal geometry of the $Mo^{IV}OS_4$ unit.

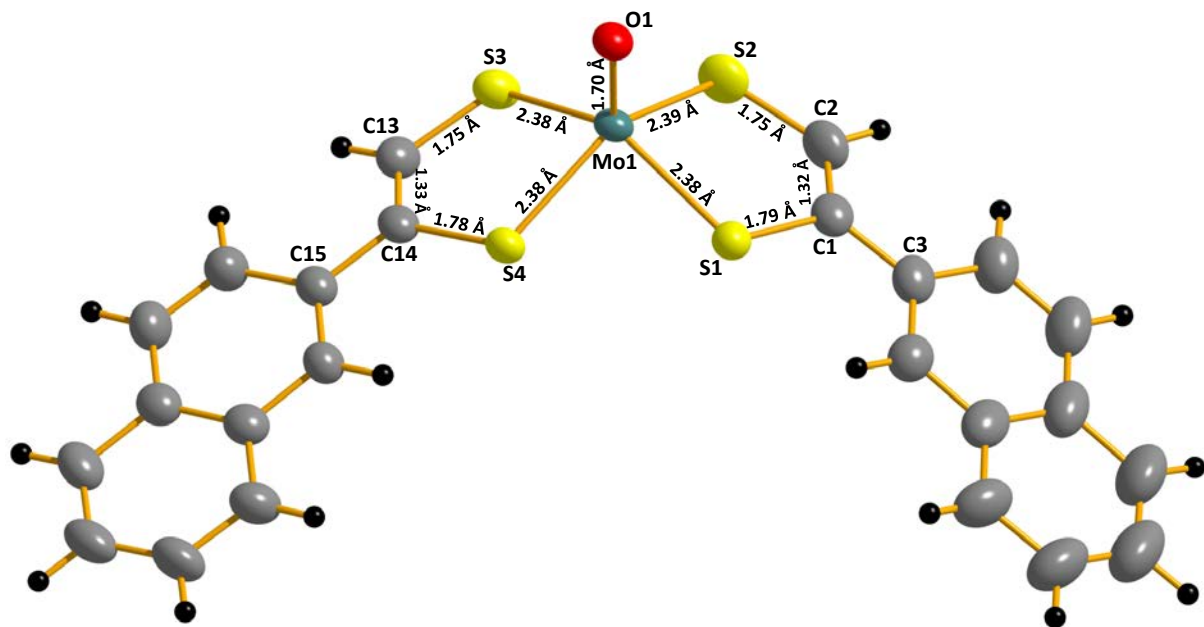


Figure S3. Molecular structure of the dianion of $[\text{Bu}_4\text{N}]_2[\text{MoO}(\text{ntdt})_2]$ (**1**) showing the bond lengths in angstrom for the MoOS_4C_4 structural motif.

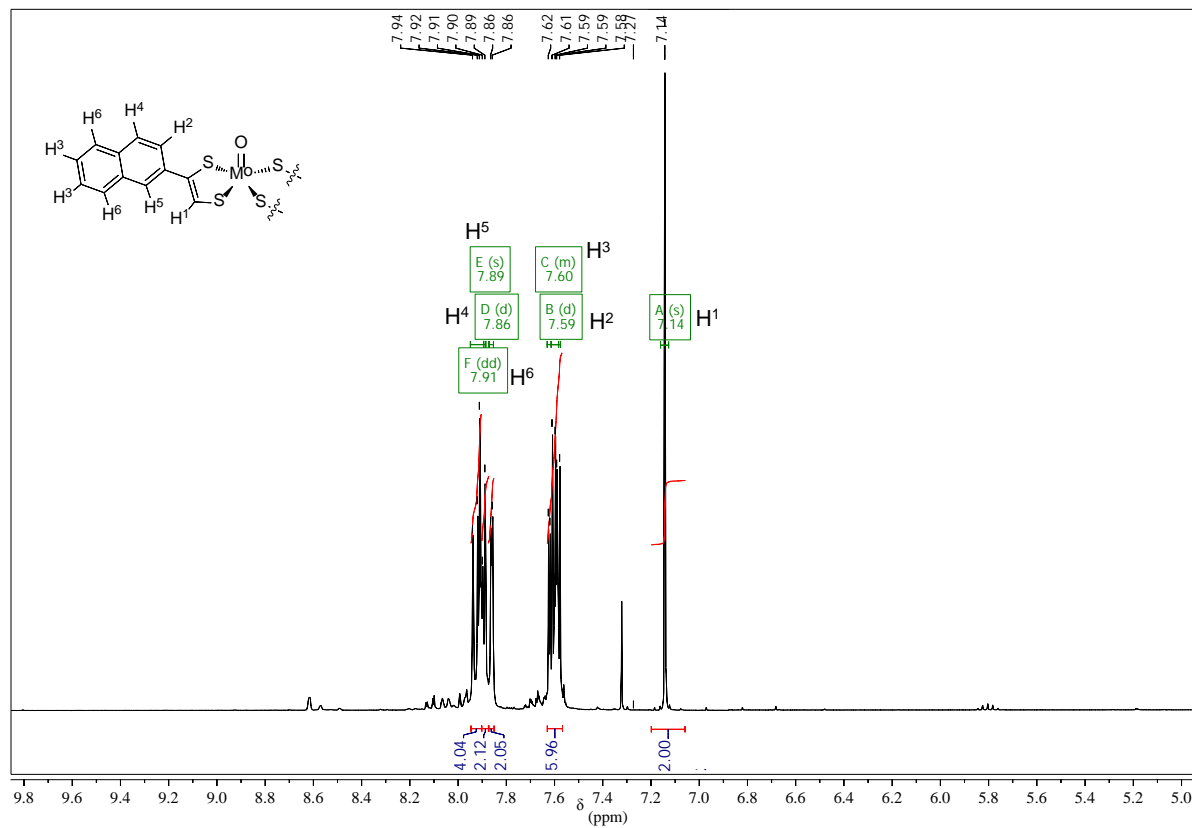


Figure S4. The 300 MHz ^1H NMR spectrum of compound **1** in CDCl_3 in the aromatic region.

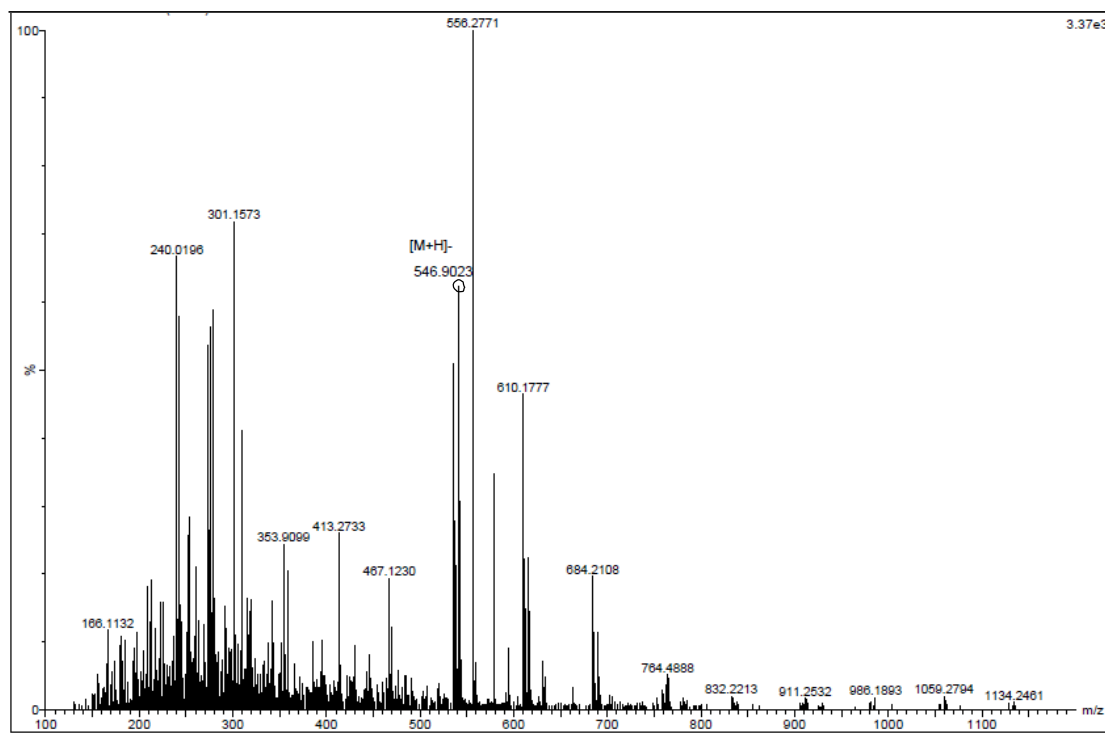


Figure S5. ESI MS spectrum from dissolution of $(\text{Bu}_4\text{N})_2[\text{MoO}(\text{ntdt})_2]$ in acetonitrile showing its $[\text{M}+\text{H}]^-$ cation adduct at m/z 546.90.

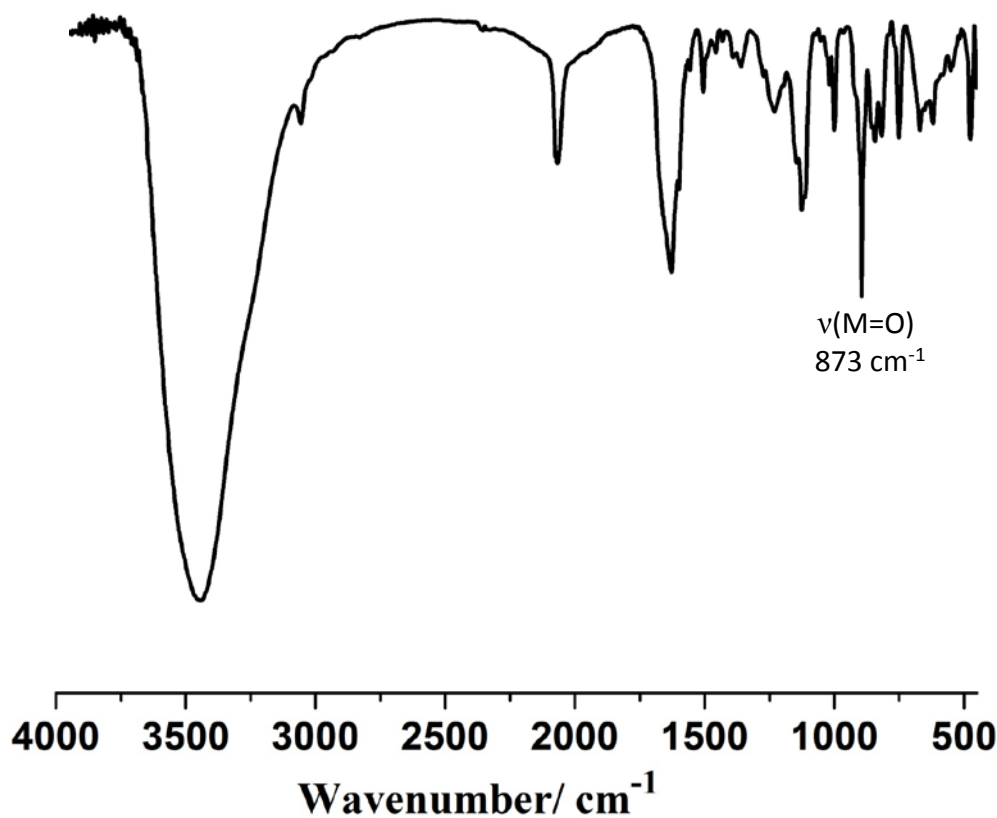


Figure S6. IR spectrum of $(\text{Bu}_4\text{N})_2[\text{MoO}(\text{ntdt})_2]$ recorded in KBr Pellets showing the $\nu(\text{Mo=O})$ at 873 cm^{-1} .

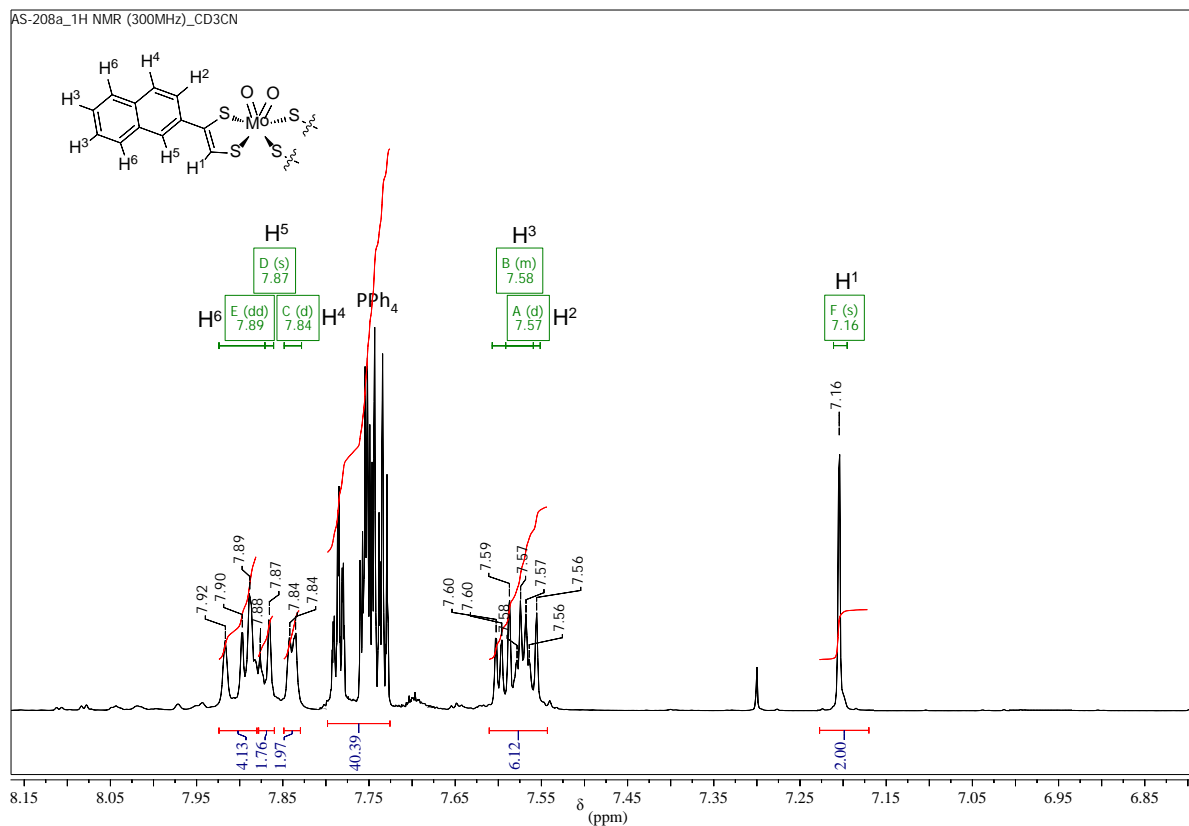


Figure S7. The 300 MHz ¹H NMR spectrum of compound **2** in CD₃CN in the aromatic region.

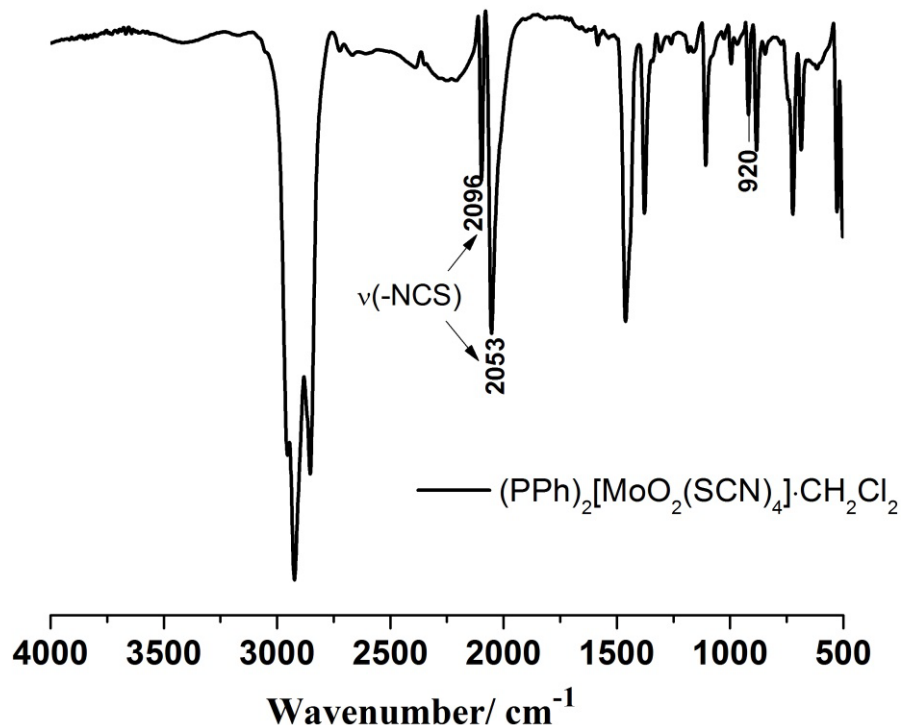


Figure S8. IR spectrum of (PPh₄)₂[MoO₂(SCN)₄] recorded in KBr Pellets showing the ν(-NCS) bands (at 2096 cm⁻¹ and 2053 cm⁻¹) and ν(Mo=O) at 920 cm⁻¹.

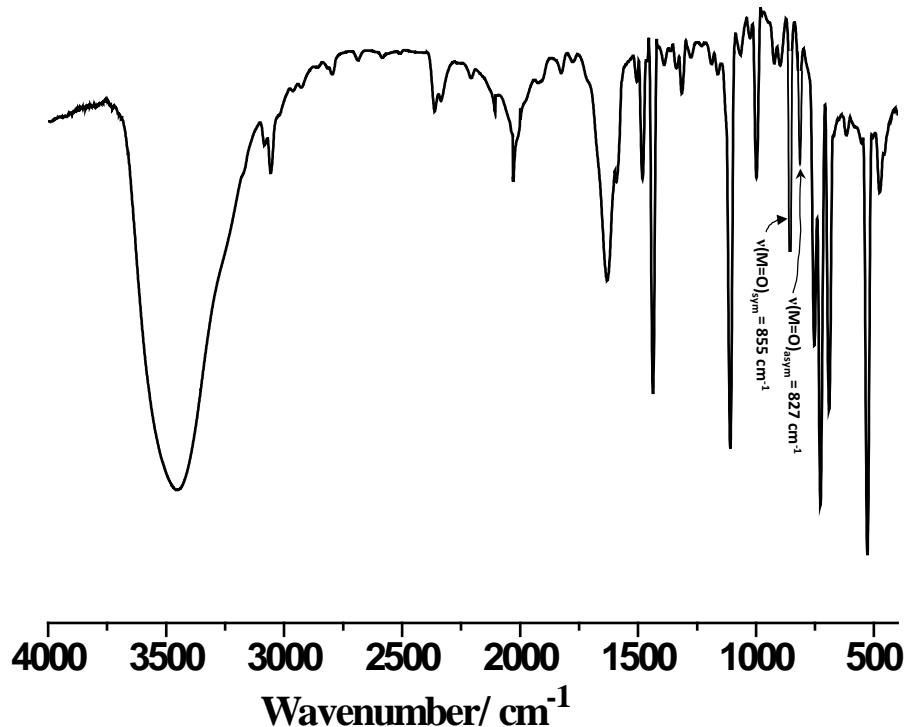


Figure S9. IR spectrum of compound **2** recorded in KBr Pellets showing the $\nu(\text{Mo=O})_{\text{sym}}$ at 855 cm^{-1} and $\nu(\text{Mo=O})_{\text{asym}}$ at 827 cm^{-1} .

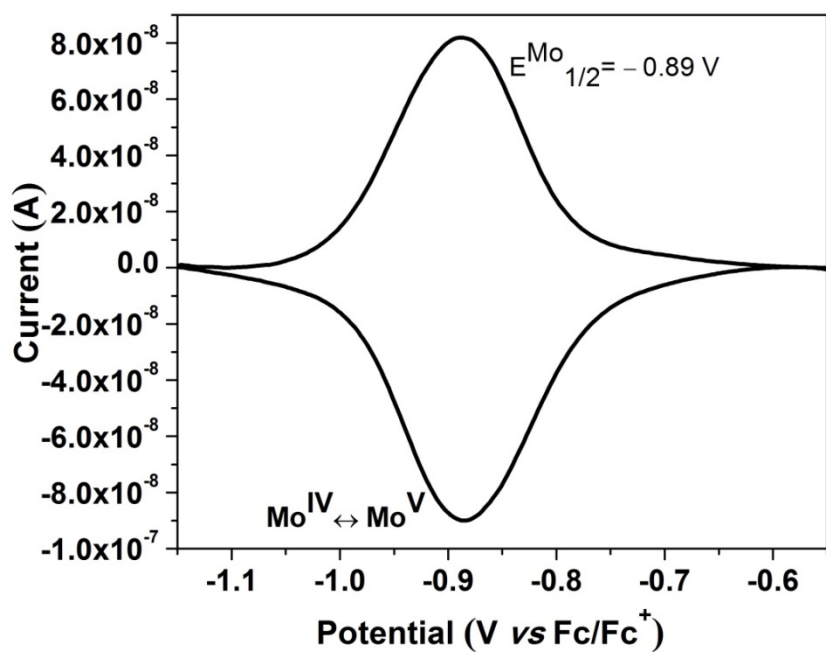


Figure S10. Differential pulse voltammogram (DPV) of compound **1** in CH_3CN containing $0.1 \text{ M } \text{Bu}_4\text{NPF}_6$. The peak potentials were recorded vs internal reference $[\text{Fc}]/[\text{Fc}]^+$ at 298 K.

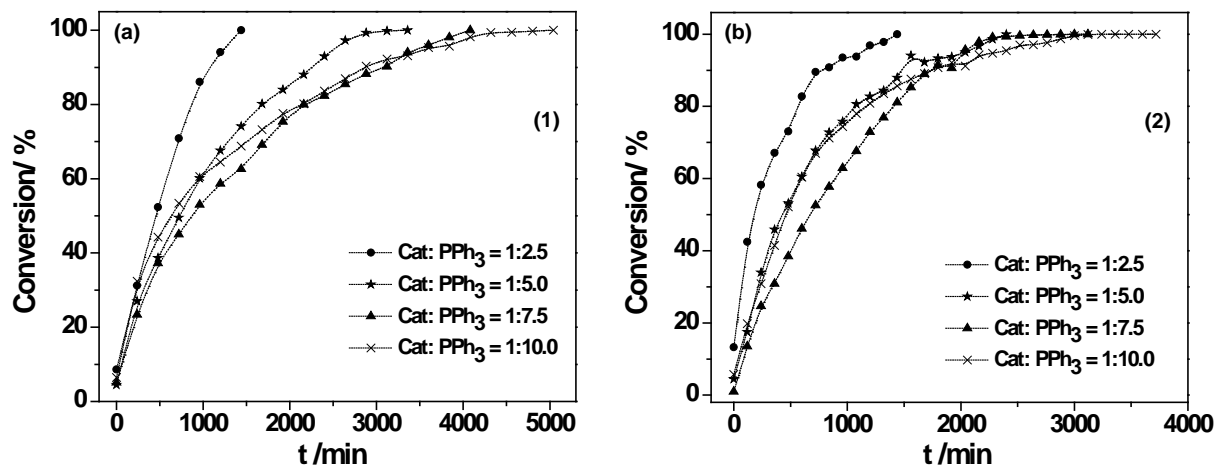


Figure S11. Conversion of PPh_3 oxidized by DMSO with time with different catalyst: PPh_3 molar ratios (a) for complex **1**, (b) for complex **2**.

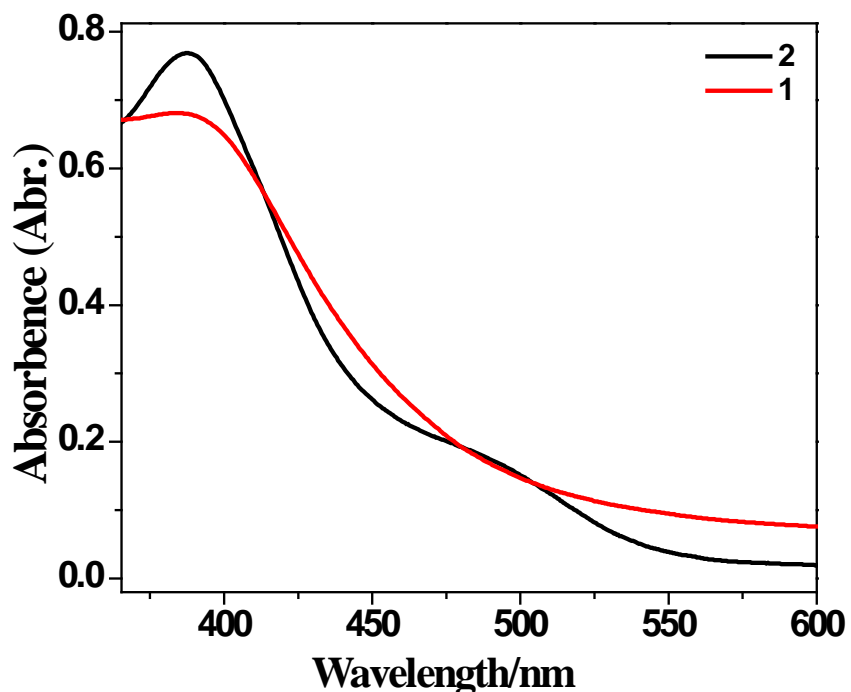


Figure S12. UV-Vis spectra of compounds **1** and **2** ($c = 1 \times 10^{-4}$) in acetonitrile at 25 °C.

Table S2. Full list of bond distances [Å] and angles [°] for $[Bu_4N]_2[MoO(ntdt)_2]$ (1).

Distance, Å			
Mo1-O1	1.7023(17)	Mo1-S4	2.3771(8)
Mo1-S3	2.3822(8)	Mo1-S1	2.3823(8)
Mo1-S2	2.3877(8)	S1-C1	1.787(3)
S2-C2	1.748(3)	S3-C13	1.745(3)
S4-C14	1.782(3)	N1-C29	1.516(3)
N1-C33	1.521(3)	N1-C25	1.521(3)
N1-C37	1.522(3)	N2-C45	1.514(3)
N2-C41	1.515(4)	N2-C49	1.523(4)
N2-C53	1.526(3)	C1-C2	1.319(4)
C1-C3	1.479(4)	C3-C4	1.388(5)
C3-C12	1.425(4)	C4-C5	1.416(4)
C5-C10	1.421(5)	C5-C6	1.431(6)
C6-C7	1.371(5)	C7-C8	1.385(7)
C8-C9	1.394(8)	C9-C10	1.418(5)
C10-C11	1.431(6)	C11-C12	1.354(5)
C13-C14	1.335(4)	C14-C15	1.490(4)
C15-C16	1.365(4)	C15-C24	1.429(4)
C16-C17	1.431(4)	C17-C18	1.404(4)
C17-C22	1.408(4)	C18-C19	1.372(4)
C19-C20	1.403(5)	C20-C21	1.359(5)
C21-C22	1.440(4)	C22-C23	1.401(4)
C23-C24	1.368(4)	C25-C26	1.529(4)
C26-C27	1.532(4)	C27-C28	1.494(5)
C29-C30	1.517(4)	C30-C31	1.533(4)
C31-C32	1.518(4)	C33-C34	1.526(4)
C34-C35	1.518(4)	C35-C36	1.518(4)
C37-C38	1.510(4)	C38-C39	1.515(4)
C39-C40	1.523(4)	C41-C42	1.520(4)
C42-C43	1.512(4)	C43-C44	1.513(4)
C45-C46	1.504(4)	C46-C47	1.528(4)
C47-C48	1.514(4)	C49-C50	1.520(4)
C50-C51	1.527(4)	C51-C52	1.519(6)
C53-C54	1.506(4)	C54-C55	1.494(5)
C55-C56	1.518(5)		
Angles, deg			
O1-Mo1-S4	108.31(6)	O1-Mo1-S3	109.46(6)
S4-Mo1-S3	82.93(2)	O1-Mo1-S1	110.59(6)
S4-Mo1-S1	84.98(3)	S3-Mo1-S1	139.94(3)
O1-Mo1-S2	108.43(7)	S4-Mo1-S2	143.25(3)
S3-Mo1-S2	85.02(3)	S1-Mo1-S2	82.28(3)
C1-S1-Mo1	108.29(10)	C2-S2-Mo1	106.68(11)

C13-S3-Mo1	106.42(10)	C14-S4-Mo1	107.38(9)
C29-N1-C33	111.33(19)	C29-N1-C25	111.2(2)
C33-N1-C25	106.39(19)	C29-N1-C37	105.70(18)
C33-N1-C37	111.61(19)	C25-N1-C37	110.66(19)
C45-N2-C41	111.3(2)	C45-N2-C49	106.6(2)
C41-N2-C49	110.5(2)	C45-N2-C53	110.2(2)
C41-N2-C53	107.05(19)	C49-N2-C53	111.3(2)
C2-C1-C3	124.3(3)	C2-C1-S1	117.9(2)
C3-C1-S1	117.5(2)	C1-C2-S2	124.1(2)
C4-C3-C12	118.3(3)	C4-C3-C1	120.8(3)
C12-C3-C1	120.9(3)	C3-C4-C5	122.2(3)
C4-C5-C10	118.8(4)	C4-C5-C6	121.9(3)
C10-C5-C6	119.3(3)	C7-C6-C5	119.7(4)
C6-C7-C8	121.7(5)	C7-C8-C9	120.2(4)
C8-C9-C10	120.2(5)	C9-C10-C5	118.9(4)
C9-C10-C11	123.1(4)	C5-C10-C11	118.0(3)
C12-C11-C10	122.0(4)	C11-C12-C3	120.7(4)
C14-C13-S3	123.4(2)	C13-C14-C15	123.7(2)
C13-C14-S4	118.6(2)	C15-C14-S4	117.5(2)
C16-C15-C24	117.1(3)	C16-C15-C14	122.1(2)
C24-C15-C14	120.8(3)	C15-C16-C17	123.0(3)
C18-C17-C22	119.8(3)	C18-C17-C16	122.3(3)
C22-C17-C16	117.9(3)	C19-C18-C17	120.0(3)
C18-C19-C20	121.6(3)	C21-C20-C19	119.4(3)
C20-C21-C22	121.0(3)	C23-C22-C17	119.5(3)
C23-C22-C21	122.2(3)	C17-C22-C21	118.3(3)
C24-C23-C22	120.8(3)	C23-C24-C15	121.6(3)
N1-C25-C26	114.7(2)	C25-C26-C27	111.5(2)
C28-C27-C26	114.6(3)	N1-C29-C30	115.7(2)
C29-C30-C31	110.3(2)	C32-C31-C30	113.7(2)
N1-C33-C34	115.1(2)	C35-C34-C33	109.8(2)
C34-C35-C36	112.8(3)	C38-C37-N1	116.8(2)
C37-C38-C39	110.0(2)	C38-C39-C40	112.9(2)
N2-C41-C42	113.9(2)	C43-C42-C41	111.4(2)
C42-C43-C44	110.9(2)	C46-C45-N2	116.6(2)
C45-C46-C47	109.8(2)	C48-C47-C46	112.7(3)
C50-C49-N2	114.5(2)	C49-C50-C51	112.1(3)
C52-C51-C50	113.9(3)	C54-C53-N2	115.6(2)
C55-C54-C53	112.6(3)	C54-C55-C56	112.6(3)